Electronic Supplementary Material (ESI) for Journal of Materials Chemistry A.

Supporting Information

WO_3 Photoanodes with Controllable Bulk and Surface Oxygen Vacancies for Photoelectrochemical Water Oxidation

Jijie Zhang, Xiaoxia Chang, Chengcheng Li, Ang Li, Shanshan Liu, Tuo Wang, and Jinlong Gong*

Key Laboratory for Green Chemical Technology of Ministry of Education, School of Chemical Engineering and Technology, Tianjin University; Collaborative Innovation Center of Chemical Science and Engineering, Tianjin 300072, China

* E-mail: jlgong@tju.edu.cn; FAX: +86-22-87401818

Experimental Section

Materials: Tungstic acid (H_2WO_4, GR, 99.0%) and hydrogen peroxide (H_2O_2, AR, 30%) were purchased from Sinopharm Chemical Reagent Co., Ltd. Polyvinyl alcohol (PVA, 97%) was supplied by Tianjin YuanLi Chemical Technology Co., Ltd. Urea (GR, 99.0%) was supplied by Kermel Chemical Technology Co., Ltd. Acetonitrile (AR, 99.0%), oxalic acid (AR, 98.0%), hydrochloric acid (HCl, 36.5-38.0 wt%), sodium sulfite (GR, 98.0%), and sodium sulfate (Na_2SO_4, GR, 99.0%) were all purchased from Tianjin GuangFu Chemical Research Institute. All the reagents were used without any purification process. High purity water (18.25 MΩ•cm) supplied by a UP Water Purification System was used in the whole experimental processes. FTO substrates (F:SnO_2, 14 Ω per square) were purchased from Nippon Sheet Glass, Japan. And before using, the FTO substrates were ultrasonically cleaned for 30 min each in deionized water, ethanol, and acetone, respectively.

Characterization: X-ray diffraction patterns were recorded with a Bruker D8 Focus operating at 40 kV and 40 mA equipped with a nickel-filtered Cu Kα radiation (λ = 1.54056 Å) and operating in a 2θ range of 20-70 ° at a scan rate of 8 per minute. The morphologies were characterized by field emission scanning electron microscope (FESEM, S-4800). TEM was performed on a JEOL JEM 2100F electron microscope operating at 200 kV. UV–visible reflectance spectra and transmittance spectra of Bi-based electrode were obtained on a HITACHI U-4100 spectrophotometer. XPS analysis of the samples was carried out on a Physical Electronics PHI 1600 ESCA system with an Al Kα X-ray source (E = 1486.6 eV). The binding energy was calibrated using the C 1s photoelectron peak at 284.6 eV as the reference. The photoluminescence spectra was obtained using a Hitachi F-4600 fluorescence spectrophotometer with excitation of

325 nm light at ambient temperature. Raman spectra was recorded on a DXR Raman Microscope with 532 nm as the excitation wavelength.

Synthesis of pristine WO_3 nanoflakes: WO_3 nanoflakes were synthesized by a modified hydrothermal method. Briefly, a seed solution prepared by dissolving 1.25 g of H_2WO_4 and 0.5 g of poly(vinyl alcohol) (PVA) into 17 mL of H_2O_2 (30 wt %) was spin-coated onto fluorine-doped tin oxide substrates at 1000 rpm, followed by annealing at 500 °C in air for 2 h. Another H_2WO_4 solution was prepared by adding 1.25 g of H_2WO_4 and 17 mL of H_2O_2 (30 wt %) into 25 mL of H_2O and stirred at 95 °C to dissolve. This H_2WO_4 solution was then diluted to 0.05 M for the hydrothermal process. In order to prepared the hydrothermal precursor solution, 3 mL of H_2WO_4 (0.05 M), 0.02 g of oxalic acid, 0.02 g of urea, 12.5 mL of acetonitrile, and 0.5 mL of HCl (6 M) were added into a 50 mL breaker and stirred to clear. An FTO substrate precoated with WO_3 seed was placed into a 50 mL Teflon-lined stainless steel autoclave filled with the as-prepared precursor solution, which was then kept at 180 °C for 2 h. Finally, the obtained sample was annealed at 500 °C in air for 2 h.

Synthesis of hydrogen-treated WO_3 nanoflakes (H-WO_3): Hydrogen treatment was carried out in a home built tube furnace system. The calcinated WO_3 nanoflake films were further annealed in hydrogen (60 sccm H_2 flow) at different time in 350 °C for the range of 10-60 minutes.

Synthesis of ozone-treated WO_3 nanoflakes (O-WO_3): Ozone treatment was also carried out in a home built tube furnace system. The calcinated WO_3 nanoflake and hydrogen-treated WO_3 films were further annealed in ozone (40 sccm O_3 flow) at different time in 100 °C for the range of 10-60 minutes.

Synthesis of WO_3 nanoflakes with annealing in hydrogen and then in ozone (HO-WO_3): The optimized WO_3 nanoflake photoelectrodes were prepared by annealing in hydrogen (60 sccm H_2 flow) in 350 °C for 30 minutes and then in ozone (40 sccm O_3 flow) in 100 °C for 30 minutes.

Photoelectrochemical Measurements: PEC measurements were performed in 0.1 M Na_2SO_4 (pH 6.8) using a standard quartz 3-electrode cell with Pt foil as the counter electrode, Ag/AgCl as the reference electrode and the WO_3 nanoflake phototelectrodes as the working electrode. In order to simulate sunlight, a 300 W xenon lamp (PE300BUV, CERMAX) equipped with an AM 1.5 filter was used as the light source, and the power intensity of the light was calibrated to 100 mW/cm^2. An electrochemical workstation (IVIUM CompactStat.e20250) was used to measure the current-voltage (I-V) characteristic of the electrode, with a scan rate of 50 mV s^{-1}. We also measure the I-V curves of the three samples under visible light irradiation with wavelength≥420 nm (**Figure S2**). Before the test, the electrode was encapsulated by epoxy and covered with a mask to expose 0.28 cm^{-2} surface area to the irradiation.

Detection of the amount of hydrogen and oxygen evolution: To quantitatively determine the amount of H_2 and O_2 produced from the reduction of water, a three-electrode system was employed. An aqueous Na_2SO_4 (0.1 M, pH 6.8) was used as the electrolyte solution. The sample was irradiated under visible light illumination (λ≥420 nm) (100 mW cm^{-2}). The gas collected from the platinum counter electrode was analyzed by an online gas chromatograph (GC2060, Shanghai RuiMin Electronics Group) with a thermal conductivity detector (TCD) using He as the carrier gas. For this purpose, a customer-designed air-tight PEC cell was used and the amount of H_2 and O_2 was measured every 1 h at a constant bias of 1.23 V *vs.* RHE under visible light illumination (λ≥420 nm).

Calculation of the incident photon to current conversion efficiency (IPCE): IPCE of the samples was acquired according to the equation:

$$IPCE\ (\%)=(I/P) \times (1240/\lambda) \times 100$$

Where I is photocurrent density at the measurement applied bias, λ is the wavelength, and P is the incident light intensity of 100 mW cm^{-2} (AM 1.5G).

Calculation of the absorbed photon to current conversion efficiency (APCE):APCE of the samples was obtained according to the equation:

$$APCE\ (\%)=\varphi_{inj} \times \eta_{cc} =[IPCE/(1-10^{-A_\lambda})] \times 100$$

Where φ_{inj} is electron-injection efficiency, η_{cc} is charge collection efficiency, and A_λ corresponds to the absorbance of the material at any particular wavelength (λ) as measured through UV-visible spectra.

Calculation of the applied bias photon-to-current efficiency (ABPE): ABPE of the three Bi-based samples was calculated according to the equation:

$$ABPE = I\times(1.23-V)/P_{light}$$

Where I is photocurrent density at the measurement applied bias, V is the applied bias (*vs.* RHE), and P_{light} is the incident light intensity of 100 mW cm^{-2} (AM 1.5G). In 0.1 M Na_2SO_4 electrolyte, the reversible hydrogen electrode (RHE) potential can be converted from the Ag/AgCl reference electrode as:

$E_{RHE} = E_{Ag/AgCl}+0.059\times pH+ E^{o}_{Ag/AgCl}$, where $E^{o}_{Ag/AgCl} = 0.197$ V at 25 ºC

Calculation of the carrier density:

The carrier density is calculated with the following equation:

$N_d=(2/e\varepsilon\varepsilon_0)[d(1/C^2)/dV]^{-1}$

Where N_d is the carrier density, e = 1.60 × 10^{-19} C is the electron charge, ε = 80 is the dielectric constant of WO_3, ε_0 = 8.85 × 10^{-14} F cm^{-1} is the vacuum permittivity, C is the capacitance of the space charge region, and V is the electrode applied potential.

The efficiency of charge separation in the bulk and on the surface

The photocurrent density arising from PEC performance (J_{PEC}) can be described as following:

$J_{PEC} = J_{abs} \times \eta_{bulk} \times \eta_{surface}$

Where J_{abs} is the photocurrent density when completely converting the absorbed photons into current (APCE = 100%). Adding 1.0 M Na_2SO_3 as the electrolyte can largely suppress the surface recombination of charge carriers without influencing the charge separation in the electrode bulk ($\eta_{surface}$ could be regarded as 100%). Therefore, η_{bulk} and $\eta_{surface}$ can be determined as following:

$\eta_{bulk} = J_{sulfite} / J_{abs}$

$\eta_{surface} = J_{water} / J_{sulfite}$

where J_{water} and $J_{sulfite}$ is the photocurrent density for PEC water oxidation and sulfite oxidation, respectively. According to the UV-vis absorptance spectrum (Fig. 2d) and the AM 1.5G solar spectrum, assuming APCE = 100%, the J_{abs} of WO_3 sample was calculated to 2.5 mA cm^{-2}. Because the UV-vis absorptance spectrum of the four samples are similar, the J_{abs} can be estimated as a constant. Therefore, the efficiency of charge separation in the bulk and on the surface of the photoelectrodes can be calculated.

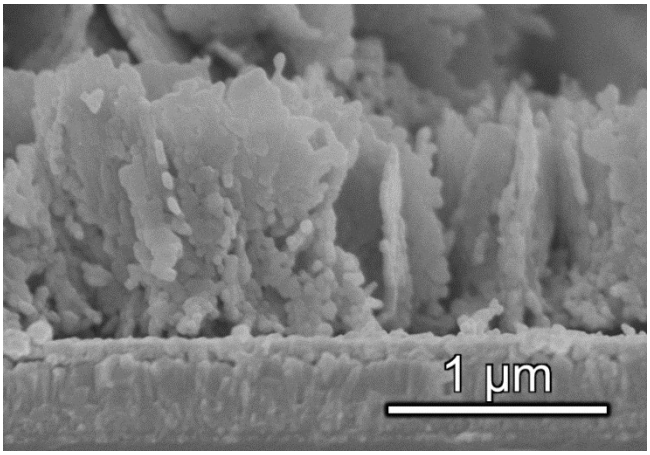

Fig. S1. Cross-sectional FESEM images of HO-WO_3 sample.

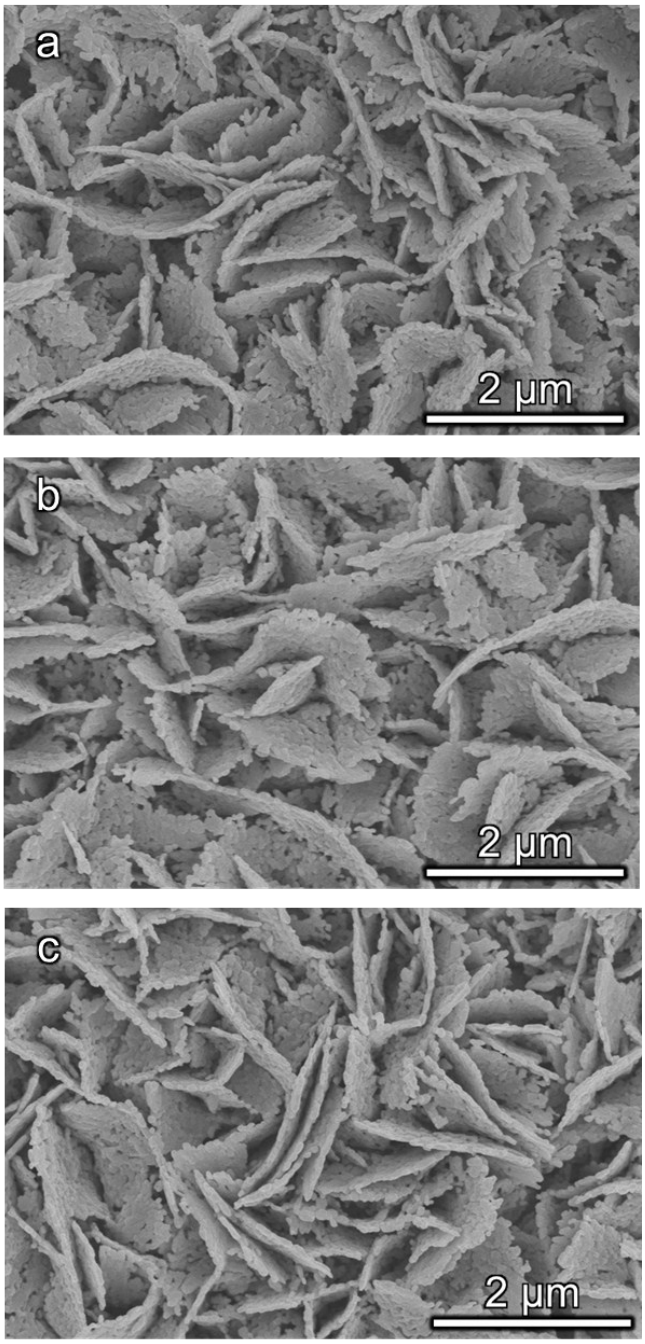

Fig. S2. SEM images of (a) WO_3, (b) H-WO_3 and (c) O-WO_3 samples.

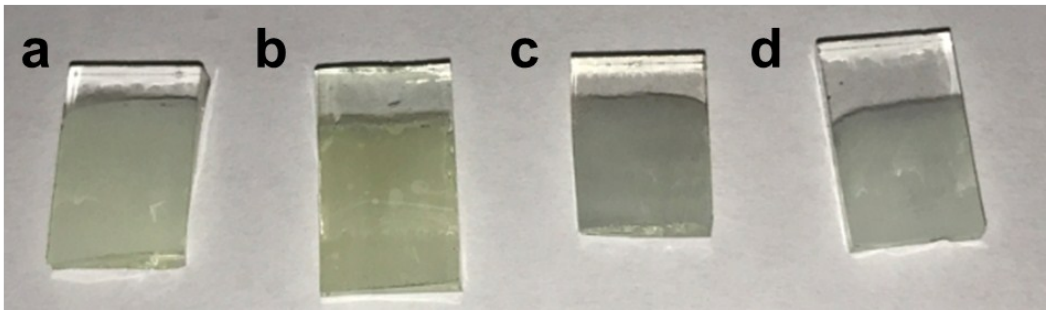

Fig. S3. Digital pictures of these samples for (a) pristine WO_3, (b) O-WO_3, (c) H-WO_3, and (d) HO-WO_3.

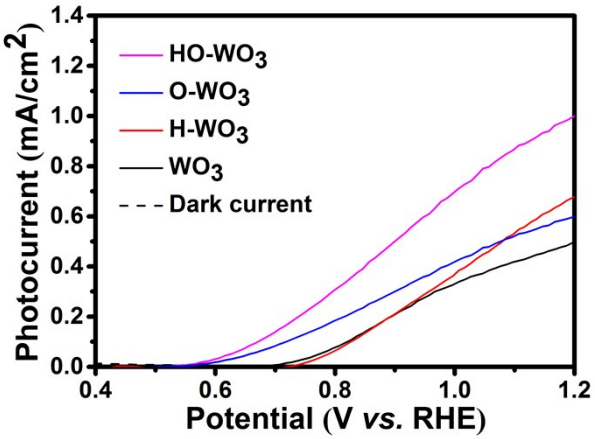

Fig. S4. Current-potential plots for pristine WO_3, H-WO_3, O-WO_3, and HO-WO_3 under visible light illumination with wavelength ≥ 420 nm in a 0.1 M Na_2SO_4 aqueous electrolyte (pH 6.8).

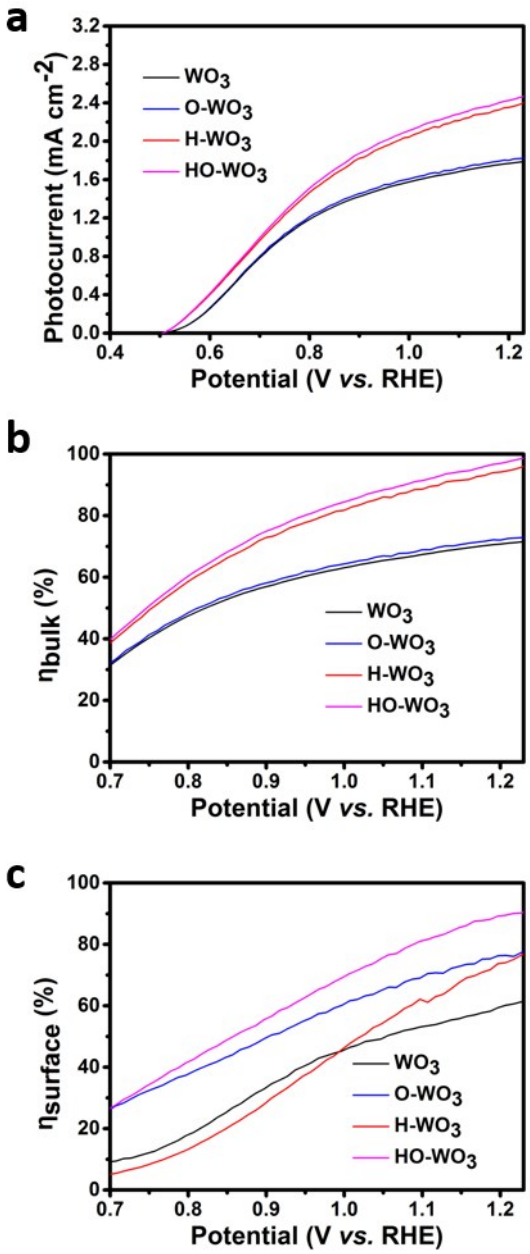

Fig. S5. (a) J-V curves of WO_3, O-WO_3, H-WO_3 and HO-WO_3 samples measured with AM 1.5G illumination (100 mW cm^{-2}) for sulfite oxidation. Charge separation efficiency (b) in the bulk (η_{bulk}) and (c) on the surface ($\eta_{surface}$) of WO_3, O-WO_3, H-WO_3 and HO-WO_3 samples.

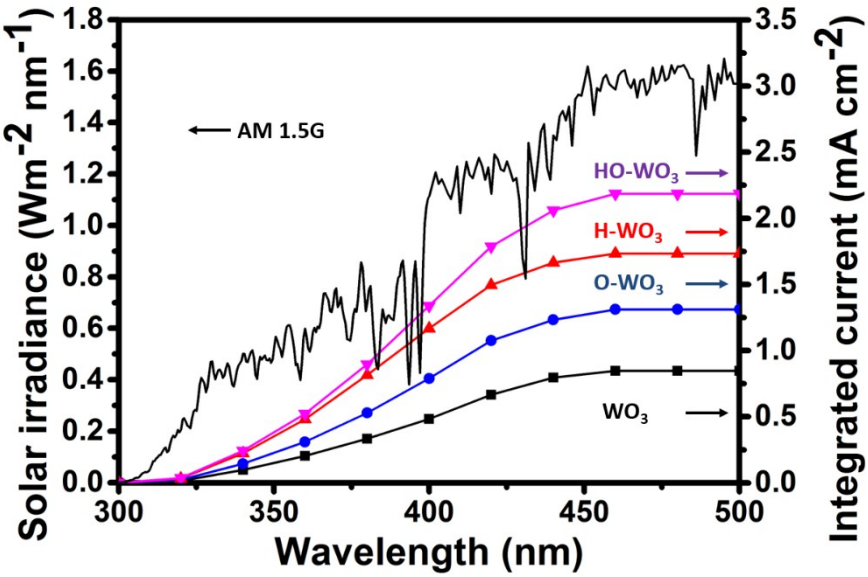

Fig. S6. Solar irradiance of standard AM 1.5G and calculated photocurrents by integrating IPCE over the photon flux of AM 1.5G of the WO_3, O-WO_3, H-WO_3 and HO-WO_3 samples at 1.23 V *vs.* RHE.

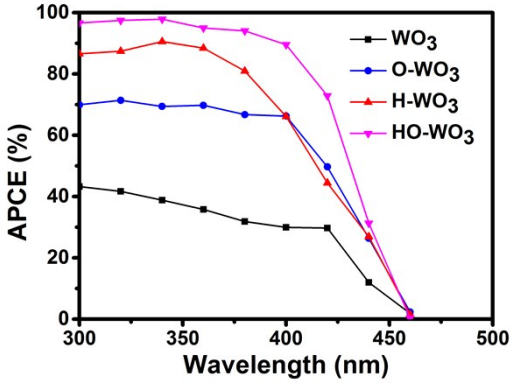

Fig. S7. APCE at different wavelengths for pristine WO_3, O-WO_3, H-WO_3, and HO-WO_3.

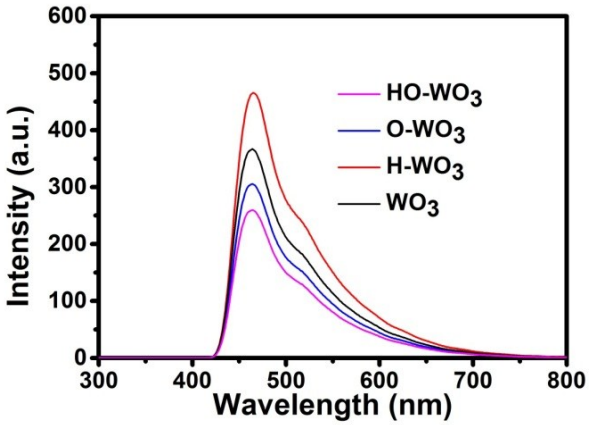

Fig. S8. PL spectra of pristine WO_3, O-WO_3, H-WO_3, and HO-WO_3.

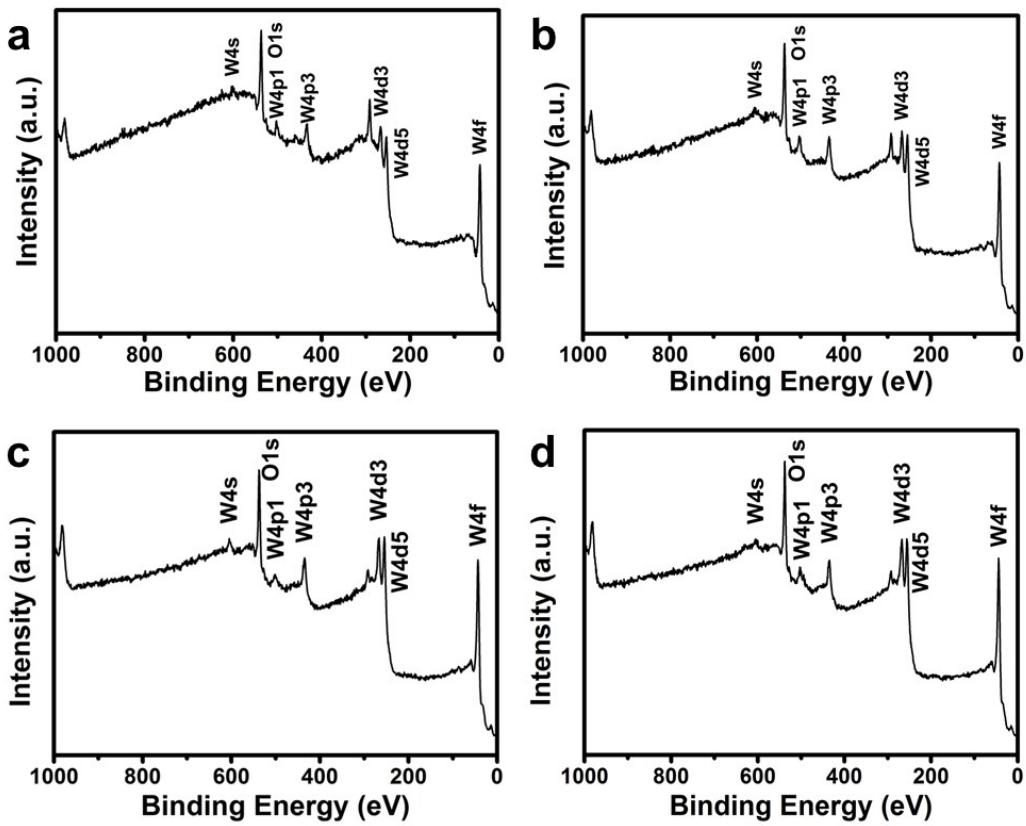

Fig. S9. XPS survey spectra collected for (a) pristine WO_3, (b) H-WO_3, (c) O-WO_3, and (d) HO-WO_3.

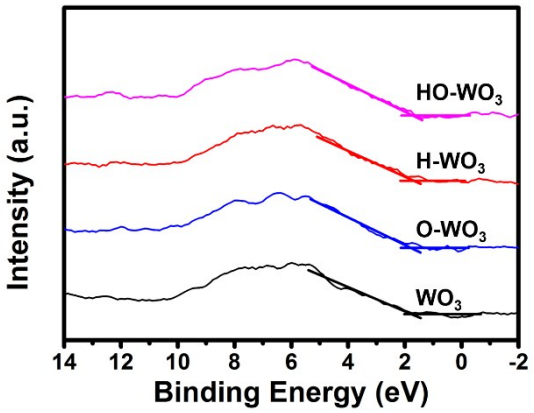

Fig. S10. XPS valence band spectra collected for pristine WO_3, O-WO_3, H-WO_3, and HO-WO_3 samples.

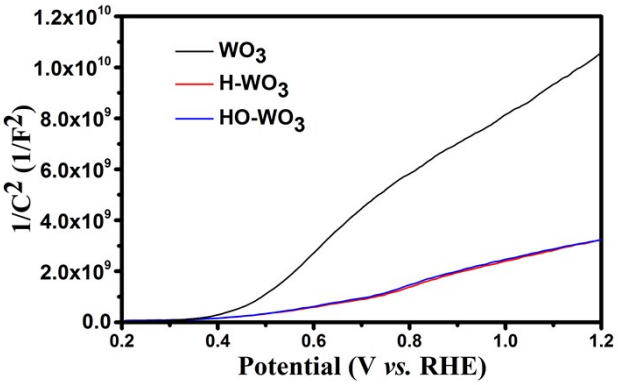

Fig. S11. Mott-Schottky plots of pristine WO_3, H-WO_3, and HO-WO_3 in a 0.1 M Na_2SO_4 aqueous electrolyte (pH 6.8).

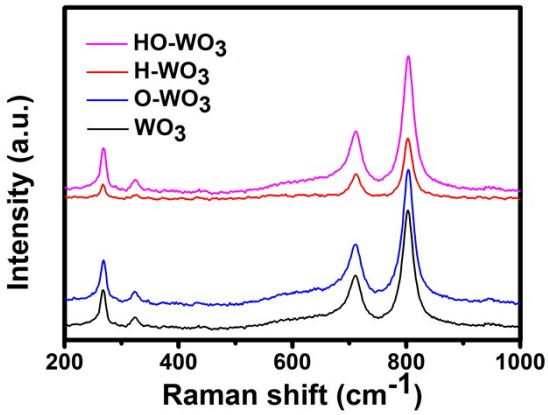

Fig. S12. Raman spectra of pristine WO_3, O-WO_3, H-WO_3, and HO-WO_3 samples.

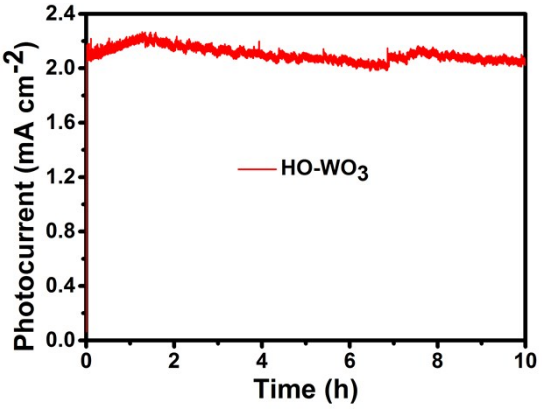

Fig. S13. A 10 h stability teat of the HO-WO_3 samples in a 0.1 M Na_2SO_4 aqueous electrolyte (pH 6.8) under AM 1.5G at a constant applied bias of 1.23 V *vs.* RHE.

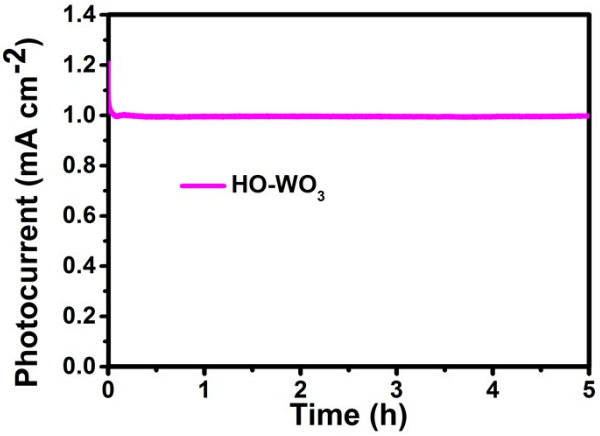

Fig. S14. Photocurrent-time plots of HO-WO_3 samples in a PEC cell under visible light irradiation ($\lambda \geq 420$ nm) in a 0.1 M Na_2SO_4 aqueous electrolyte (pH 6.8). The constant potential is 1.23 V *vs.* RHE.

Quantify the loss of oxygen evolution

We can quantify the amount of $S_2O_8^{2-}$ by detecting Fe^{3+} which is oxidized from Fe^{2+} by $S_2O_8^{2-}$ (*eq.* 3).

$$2Fe^{2+} + S_2O_8^{2-} \rightarrow 2SO_4^{2-} + 2Fe^{3+} \quad (3)$$

The characteristic peaks of Fe^{2+} and Fe^{3+} are located on 250 nm and 290 nm in UV-visible diffusive reflectance spectra. According to the absorbance of Fe^{3+}, the concentration of Fe^{3+} can be calculated. Fig. S15 shows the standard curve of $Fe_2(SO_4)_3$ solution with different concentration (10^{-3} M, 5×10^{-4} M, 10^{-4} M, and 10^{-5} M). After 5 h stability measurement, 5 mL 10^{-3} M $FeSO_4$ solution was added into 5 mL electrolyte and then this solution was stirred for 10 min. The absorbance of this solution at 290 nm is about 0.252 (Fig. S16). The concentration of $S_2O_8^{2-}$ in 5 mL electrolyte is 2.52×10^{-4} M. So the amount of $S_2O_8^{2-}$ in 50 mL electrolyte after 5 h stability measurement is 12.6 μmol. Therefore, the amount of oxygen which is calculated by $S_2O_8^{2-}$ in side reaction is 6.3 μmol.

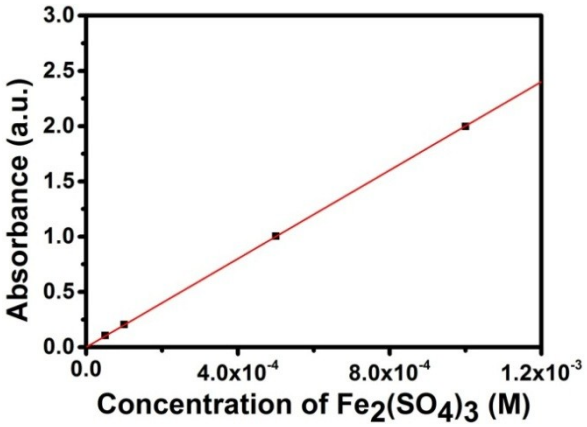

Fig. S15. The standard curve of $Fe_2(SO_4)_3$ solution with different concentration (10^{-3} M, 5×10^{-4} M, 10^{-4} M, and 10^{-5} M).

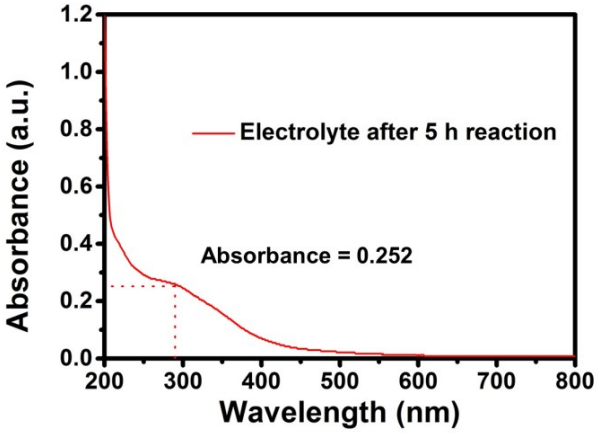

Fig. S16. UV-vis plots of electrolyte after 5 h reaction with adding 10^{-3} M $FeSO_4$ solution.

Table S1. Summary of various WO_3 photoanodes.

Ref.	Sample	Electrolyte	Photocurrent at 1.23 V *vs.* RHE (mA cm^{-2})	Onset Potential (V *vs.* RHE)	Stability
This work	WO_3 nanoflake	0.1 M Na_2SO_4 (pH=6.8)	2.25	0.57	10 h (> 95% retention)
1	$W_{1-x}O_{3-y}$	0.5 M Na_2SO_4 (pH=6.8)	2.75	0.56	10 h (73% retention)
2	WO_3 columns	0.1 M H_2SO_4 (pH=1)	2.40	0.57	0.5 h (65% retention)
3	WO_3 porous nanosheet	0.5 M Na_2SO_4	1.27	0.70	1 h (100% retention)
4	FeOOH/WO_3	0.5 M K_2SO_4 (pH=6.8)	1.50	0.70	2 h (66% retention)
5	FeOOH/WO_3	0.1 M KPi (pH=7)	1.42	0.68	3 h (100% retention)
6	WO_3 nanoflower	1 M H_2SO_4 (pH=0)	1.10	0.63	2 h (50% retention)
7	IrO_2/WO_3	1 M H_2SO_4 (pH=0)	1.00	0.65	N/A
8	N-doped WO_3	0.5 M H_2SO_4 (pH=0.3)	2.61	0.59	N/A
9	WO_{3-x}	0.5 M Na_2SO_4	0.52	0.70	7 h (80% retention)
10	WO_3 nanoplate	0.5 M Na_2SO_4	0.25	0.68	140 s (90% retention)

Notes and references

1. M. Ma, K. Zhang, P. Li, M. S. Jung, M. J. Jeong, J. H. Park, *Angew. Chem. Int. Ed.* 2016, *55*, 11819-11823.
2. C. Fàbrega, S. Murcia-López, D. Monllor-Satoca, J. D. Prades, M. D. Hernández-Alonso, G. Penelas, J. R. Morante, T. *Andreu, Appl. Catal., B* 2016, *189*, 133-140.
3. Y. Liu, L. Liang, C. Xiao, X. Hua, Z. Li, B. Pan, Y. Xie, *Adv. Energy Mater.* 2016, *6*, 1600437.
4. W. L. Kwong, C. C. Lee, J. Messinger, *J. Phys. Chem. C* 2016, *120*, 10941-10950.
5. J. W. Huang, Y. Ding, X. Luo, Y. Y. Feng, *J. Catal.* 2016, *333*, 200-206.
6. N. Wang, D. Wang, M. Li, J. Shi, C. Li, *Nanoscale* 2014, *6*, 2061-2066.
7. J. M. Spurgeon, J. M. Velazquez, M. T. McDowell, *Phys. Chem. Chem. Phys.* 2014, *16*, 3623-3631.
8. Y. Liu, Y. Li, W. Li, S. Han, C. Liu, *Appl. Surf. Sci.* 2012, *258*, 5038-5045.
9. G. Wang, Y. Ling, H. Wang, X. Yang, C. Wang, J. Z. Zhang, Y. Li, *Energy Environ. Sci.* 2012, *5*, 6180.
10. J. Y. Zheng, G. Song, J. Hong, T. K. Van, A. U. Pawar, D. Y. Kim, C. W. Kim, Z. Haider, Y. S. Kang, *Cryst. Growth Des.* 2014, *14*, 6057-6066.